Supporting Information

An Electrochemical Strategy using Multifunctional Nanoconjugates for Efficient Simultaneous Detection of *Escherichia coli* O157:H7 and *Vibrio cholerae* O1

Yan Li,[1] Ya Xiong,[3] Lichao Fang,[1] Lili Jiang,[1] Hui Huang,[1] Jun Deng,[1] Wenbin Liang,[1, 2, *] Junsong Zheng[1, *]

[1]Department of Clinical Laboratory Science, College of Medical Laboratory, Southwest Hospital, Third Military Medical University, 30 Gaotanyan Street, Shapingba District, Chongqing 400038, PR China

[2]Department of Clinical Biochemistry, Laboratory Sciences, Southwest Hospital, Third Military Medical University, 30 Gaotanyan Street, Shapingba District, Chongqing 400038, PR China

[3]Department of Dermatology, Southwest Hospital, Third Military Medical University, 30 Gaotanyan Street, Shapingba District, Chongqing 400038, PR China

[*]Corresponding author: Junsong Zheng, Wenbin Liang

E-mail: zhengalpha@yahoo.com (J.S. Zheng); wenbinliangasu@gmail.com (W.B. Liang)

Fax: +86 23 68772700

Table of Contents

Oligonucleotides employed for the signal amplification

All oligonucleotides were custom-synthesized by Shanghai Sangon Biological Engineering Technology and Services Co., Ltd. (Shanghai, China). Sequences of the oligonucleotides are listed in Table 1. Before using, all hairpin nucleotides were heated to 95 °C for 2 min and then brought to room temperature to form stem-loop structures.

Table S1. The oligonucleotides employed for the signal amplification.

Name	Sequence (5'→3')
Nucleotide initiator 1/NI1	HS-TTT TTA GTC TAG GAT TCG GCG TGG GTT AA
Hairpin nucleotide 1/HP1	ATT CGA TCT TAA CCC ACG CCG AAT CCT AGA CTC AAA GTG ATT CGA TCA GTC TAG GAT TCG GCG TG
Hairpin nucleotide 2/HP2	ATT CGA TCA GTC TAG GAT TCG GCG TGG GTT AAA TCC TAG ACT GAT CGA ATA CTT TGT CGG CGT G
Signal probe 1/SP1	NH_2-TTT TTC ACG CCG ATG ATC GAA
Nucleotide initiator 2/NI2	HS-TTT TTC CTA GAG CTA AGC TAT GAC CTG GT
Hairpin nucleotide 3/HP3	GCT AAG CTA TGA CCT GGT CCA TGA CGA CCT TGA CCA GGT CAT AGC TTA GCT CTA GGC CAT GAC G
Hairpin nucleotide 4/HP4	GCT AAG CTC AAG GTC GTC ATG GAC CAG GTC ATC CTA GCT AAG CTA TGA CCT GGT CCA TGA CG
Signal probe 2/SP2	NH_2-TTT TTC GTC ATG GTA GCT TAG C

Characterization of HCR Amplification

In this study, the nucleotides employed for the HCR amplification were characterized by polyacrylamide gel electrophoresis (Figure S1). The molecule weights of the nucleotides were

characterized by distribution places of the UV bands from notches. As shown in Figure S1, lane 1~4 and lane a~d represented the nucleotide initiator 1 (lane 1), hairpin nucleotide 1 (lane 2), hairpin nucleotide 2 (lane 3), signal probe 1 (lane 4), nucleotide initiator 2 (lane a), hairpin nucleotide 3 (lane b), hairpin nucleotide 4 (lane c), and signal probe 2 (lane d). The HCR reaction could be triggered by nucleotide initiator with hairpin nucleotides, forming long nucleotides polymers (lane 5 and lane e). Importantly, the long nucleotides polymers with increased molecular weights could attach massive signal probes for the enhancement of electrochemical response, which was associated with the nucleotide initiator. The electrochemical response could thus be used to indicate the concentration of nucleotide initiator and associated antibodies with improved sensitivity and efficiency.

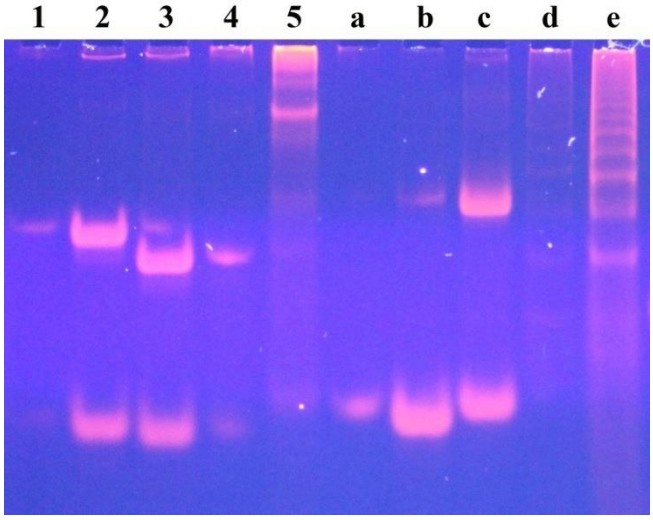

Figure S1. Polyacrylamide gel electrophoresis characterization of the nucleotides: lane 1, nucleotide initiator 1; lane 2, hairpin nucleotide 1; lane 3, hairpin nucleotide 2; lane 4, signal probe 1; lane 5, product of HCR reaction from hairpin nucleotide 1 and hairpin nucleotide 2; lane a, nucleotide initiator 2; lane b, hairpin nucleotide 3; lane c, hairpin nucleotide 4; lane d, signal probe 2; lane e, product of HCR reaction from hairpin nucleotide 3 and hairpin nucleotide 4.

Preparation of the Self-designed Magnetic Sensor

As shown in the mechanical design drawing (Figure S2), the self-designed magnetic sensor mainly included external cavity (D), retaining plate (E), retaining latch for electrode (F), glassy carbon plate (G), magnet (H), retaining latch for magnet (I) and sealing gasket (J). The bare glassy carbon plate (GCP) was polished carefully with 0.3 and 0.05 μm aluminum slurry and ultrasonicated with ethanol and water. The magnetic sensor was then assembled as shown in Figure S2B and employed for the simultaneous electrochemical assay. After each detection, the magnetic sensor could be regenerated simply by washing twice with PBS. The self-designed magnetic sensor could not only improve the feasibility of the simultaneous assay, but also enhance the analysis speed and efficiency due to the separated reaction-detection system and rapid regeneration after each detection.

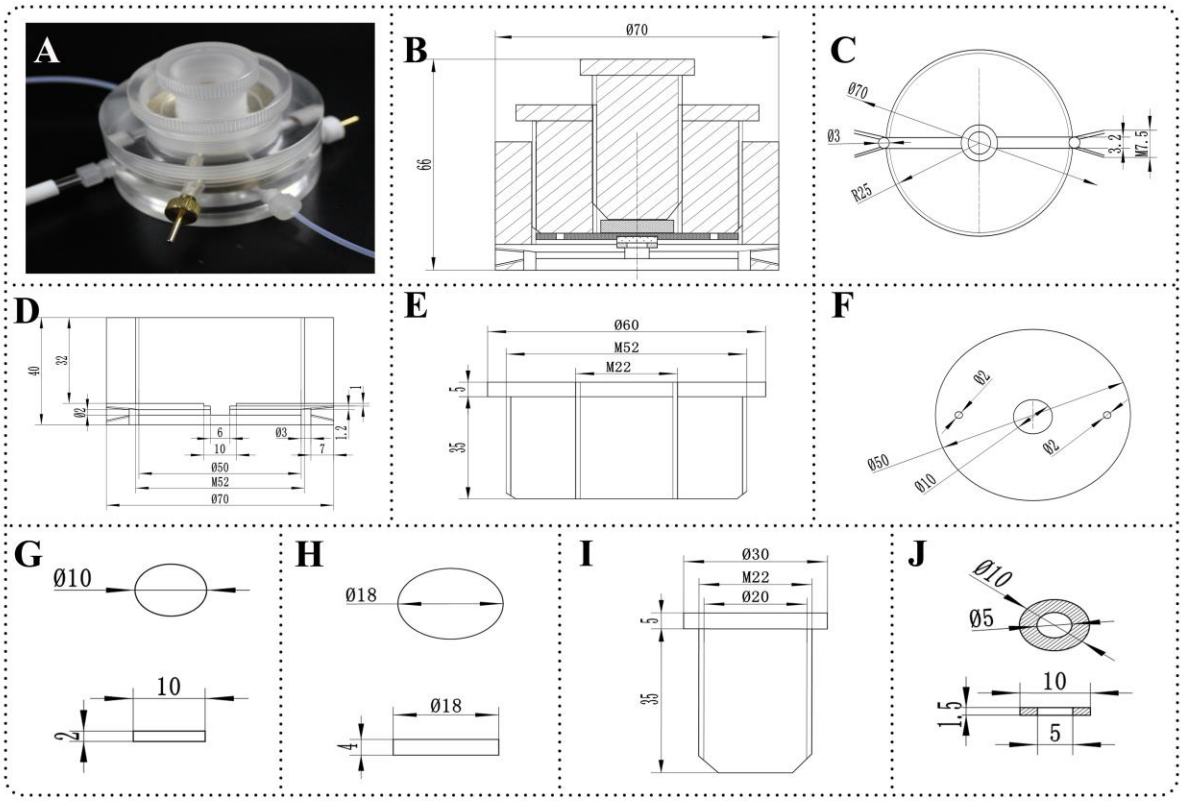

Figure S2. Photograph and mechanical design drawing of the self-designed magnetic sensor. A, photograph of the magnetic sensor; B, front view; C, top view; D, external cavity; E, retaining plate; F, retaining latch for electrode; G, glassy carbon plate; H, magnet; I, retaining latch for magnet and J, sealing gasket.

Morphology Characterization of C_{60} and C_{60}@AuNPs

In this work, scanning electron microscope (SEM) was employed to characterize the morphologies of C_{60} and C_{60}@AuNPs (Figure S3). The C_{60} showed a homogeneous and good dispersion with a globular structure (Figure S3A), which was consistent with the previous report.[S1] After the conjugation of gold nanoparticles (AuNPs) on the C_{60} surface (Figure S3B),

many small spherical bright spots with the size of about 16 nm were distributed uniformly and tightly on the C_{60} surface, indicating the successful preparation of C_{60}@AuNPs.

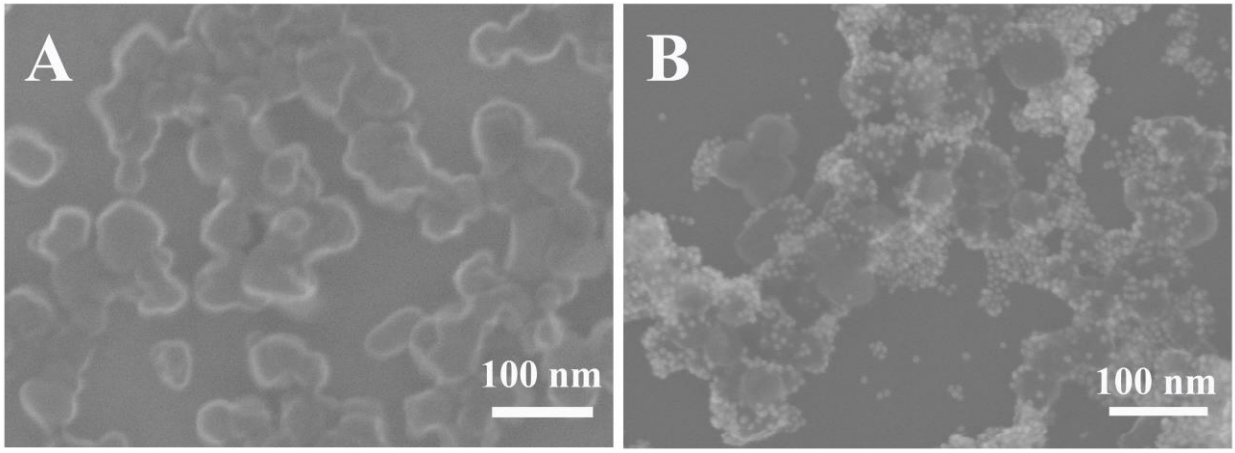

Figure S3 SEM images of (A) C_{60} and (B) C_{60}@AuNPs at an acceleration voltage of 15 kV.

Optimization of the Detection Conditions

The experimental parameters could affect the detection performance of the electrochemical assay. Herein, some important parameters were optimized based on the electrochemical determination of 1000 CFU/mL *E. coli* O157:H7, including the concentration of capture antibodies, the concentration of multifunctionalized detection antibodies, the incubation time, the incubation temperature, the concentration of hairpin nucleotides, and the time for HCR.

The effect of the different concentrations of capture antibodies on the electrochemical response was investigated from 0.1 to 50 μg/mL. As shown in Figure S4A, the current response increased rapidly with the increasing concentration of capture antibodies and then slowly leveled off after 5 μg/mL. The concentration of 5 μg/mL was therefore employed as the optimal concentration of capture antibodies.

Electrochemical responses for the different concentrations of multifunctionalized detection antibodies were performed from 0.1 to 50 μg/mL as shown in Figure S4B. The results indicated that the current signals increased rapidly with the increasing concentration of the multifunctionalized detection antibodies and reached an equilibration state after 10 μg/mL. Thus, 10 μg/mL was used as the optimized concentration of the multifunctionalized detection antibodies.

To investigate the effect of the incubation time, the proposed electrochemical assay was used for the detection of 1000 CFU/mL *E. coli* O157:H7 with incubation time from 5 to 80 min. As shown in Figure S4C, the electrochemical signals increased with longer incubation times and became steady after 40 min. Therefore, an incubation time of 40 min was employed for the electrochemical assay in this study.

The incubation temperature as an important parameter for the electrochemical assay was also investigated by performing the current response with different temperatures ranging from 17 to 60 °C. As shown in Figure S4D, the current response increased with increasing incubation temperature and reached a peak at 35 °C and then decreased quickly due to the negative effect of high temperature on the immunoreaction and HCR amplification. Although the maximum current response was obtained at 35 °C, considering the convenience of the electrochemical assay, room temperature (25 °C) was used as the incubation temperature.

The concentration of hairpin nucleotides was an important factor for the efficiency of HCR amplification, which was investigated by the current response at different concentrations of hairpin nucleotides from 0.02 to 3 μM (Figure S4E). The current signal reached a peak when the concentration of hairpin nucleotides was 1 μM indicating the optimum performance of HCR to

amplify the electrochemical response. Then the current signal decreased slowly with increasing concentration because the longer DNA sequence induced space folding and higher steric hindrance. Thus, the concentration of hairpin nucleotides of 1 μM was selected as the optimum concentration for all subsequent assays.

For the HCR amplification, the reaction time was another very important factor, which was investigated based on the electrochemical response with different HCR reaction times ranging between 5 to 70 min (Figure S4F). The current signals increased rapidly with increasing reaction time and reached an equilibration state when the reaction time was longer than 30 min. Therefore, the HCR reaction time of 30 min was used in this work.

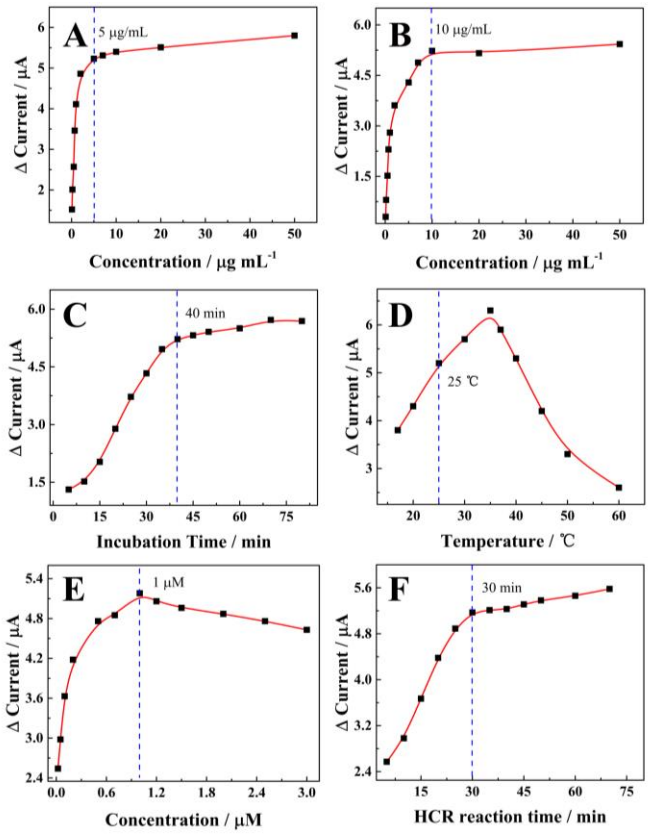

Figure S4. Optimization of the detection conditions based on the electrochemical determination of 1000 CFU/mL *E. coli* O157: H7, including (A) the concentration of capture antibodies, (B) the concentration of multi-functionalized detection antibodies, (C) the incubation time, (D) the incubation temperature, (E) the concentration of hairpin nucleotides, and (F) the reaction time for HCR amplification.

Supporting Figures.

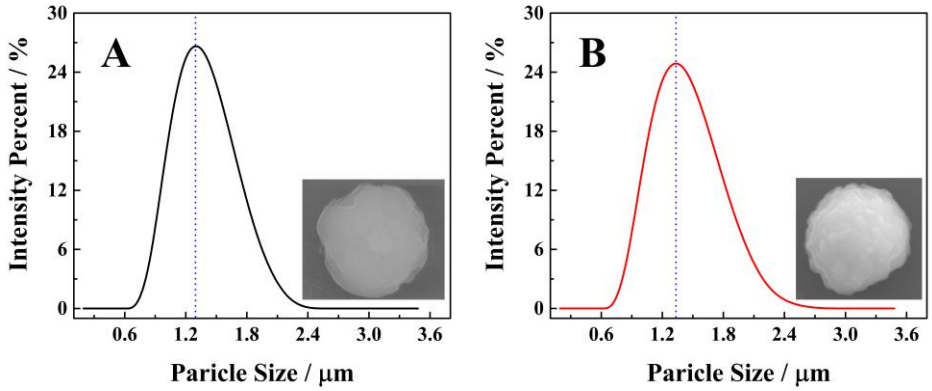

Figure S5. Particle size characterization of MB@SA (A) and MB@SA/capture antibodies (B). Inserts show the SEM images with high amplification for MB@SA (A) and MB@SA/capture antibodies (B), respectively.

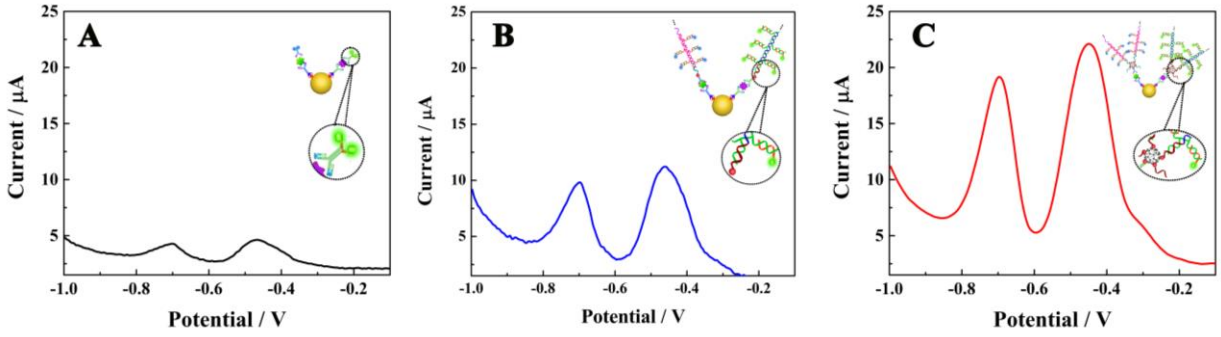

Figure S6. Characterization of the amplification efficiency based on DPV: A, CdS- or PbS-labeled antibodies without improvement of C_{60}@AuNPs as the nanocarrier and HCR amplification; B, CdS- or PbS-labeled antibodies with improvement of AuNPs as the nanocarrier and HCR amplification; C, CdS- or PbS-labeled antibodies with improvement of C_{60}@AuNPs as the nanocarrier and HCR amplification.

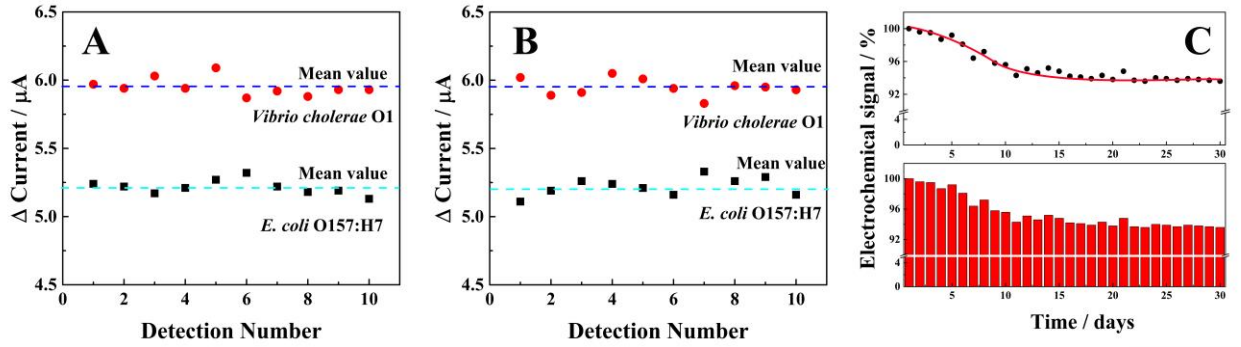

Figure S7. The reproducibility and stability characterizations of the proposed electrochemical strategy: A, investigation of the reproducibility by inter-assay; B, investigation of the reproducibility by intra-assay; C, characterization of the stability by long-term storage assay.

References

S1 Zhao M, Zhuo Y, Chai YQ, Yuan R. Au nanoparticles decorated C_{60} nanoparticle-based label-free electrochemiluminesence aptasensor via a novel “on-off-on” switch system. Biomaterials. 2015; 52: 476-83.